PERGAMON

International Journal of Multiphase Flow 25 (1999) 109–138

International Journal of Multiphase Flow

Downward bubbly gas–liquid flow in a vertical pipe

O.N. Kashinsky *, V.V. Randin

Institute of Thermophysics, 630090 Novosibirsk, Russia

Received 29 February 1996; received in revised form 28 June 1998

Abstract

Local characteristics of downward bubbly flow in a 42.3 mm i.d. vertical pipe were investigated. An electrochemical technique was used to measure wall shear stress, local void fraction, liquid velocity, wall shear stress and velocity fluctuations. A gas–liquid mixer was used permitting the change in size of gas bubbles for the same gas and liquid flow rates. Special attention was paid to measurements close to the pipe wall.

An increase of wall shear stress as compared to single-phase turbulent flow was observed. The existence of the single-phase law-of-the-wall was proved for downward flow. A comparison of upward and downward bubbly flow structure was made.

Keywords: Bubbly flow; Bubble size; Electrochemical method; Void fraction; Liquid velocity; Wall shear stress; Fluctuations

1. Introduction

The structure of gas–liquid bubbly flows in pipes has been intensively studied in the last years. Most of these investigations considered the case of cocurrent upward flow (Serizawa et al., 1975; Nakoryakov et al., 1981; Liu and Bankoff 1993; etc.). Contrary, quite little attention was paid to the study of downward bubbly flow. The first observation of the structure of this flow along with phase distribution measurements was made by Ibragimov et al. (1973). The study of downward gas–liquid flow was performed by Oshinovo and Charles (1974) and later in a series of papers by Clark and Flemmer (1984, 1985a, 1985b). Detailed experimental studies of voids and velocity profiles were made by Ganchev et al. (1984),

* Corresponding author.

0301-9322/99/$ - see front matter
PII: S0301-9322(98)00040-8

Ganchev and Peresadko (1985) and Wang et al. (1987). A complex study of flow parameters in a small diameter pipe was performed by Gorelik et al. (1987).

Theoretical predictions of void distribution in downward bubbly flows were made by Ibragimov et al. (1973), Drew and Lahey (1982), Wang et al. (1987). Both experimental and theoretical studies demonstrated that the main feature of downward flow was the concentration of the gas phase in the central part of the pipe. Quite limited information was obtained on liquid velocity distributions and the turbulent structure of the flow.

The purpose of this paper is to present detailed experimental results on the structure of cocurrent downward bubbly flow in a vertical pipe. Special attention was devoted to wall shear stress measurements and to the measurements of the flow parameters in the near-wall region of the flow which was not investigated in the previous studies.

2. Experimental technique

2.1. Experimental set-up

Experiments were made in the set-up schematically shown in Fig. 1. Test liquid was contained in storage tank (1). Liquid was pumped through the flow loop by centrifugal pump (2). Test section (8) was a vertical Plexiglas pipe of 42.3 mm inner diameter. The test section consisted of several pieces of this pipe, the total length of which was 4.8 m. At the outlet of the test section, valve (15) was mounted to adjust the pressure in the test section. The pressure was measured by a manometer (14). Gas–liquid flow from the test section entered the separator (16), after which the liquid returned to the storage tank and the gas was exhausted to the atmosphere. The liquid temperature was measured by a thermometer (18) and maintained constant by a temperature regulator (19) and a cooling coil (17). Cooling water supply to the cooling coil was controlled by an electric valve (20).

The liquid flow rate was adjusted by valves (3) and (4) and measured by rotameters (5) and an orifice meter (6) connected to a differential pressure transducer. Measurements of the local flow parameters were made in measuring units (9), (10) and (13). A pressure drop was measured by the pressure taps (11) and (12) and U-tube manometer (25).

Air from the pressure line was supplied to the mixer (7). The air flow rate was regulated by valves (21) and (24) and measured by a calibrated orifice meter (23). Air pressure before the orifice meter was measured by a manometer (22). An optical glass was mounted in the measuring unit (13) for flow observation and photography.

To produce gas–liquid flow, a special mixer (7) was mounted at the inlet of the test section. This mixer is shown in Fig. 2. Gas was supplied through a unit (6) into an annual chamber produced by the mixer body (1) and a Plexiglas tube (3). The gas was injected to the liquid through 120 holes 0.2 mm in diameter drilled in the Plexiglas tube. Gas bubbles were generated in the annular slot produced by the mixer body and a cylindrical insert (2). Liquid was pumped to the slot through unit (5). The liquid flow rate through the slot was maintained constant in the given experiment. The rest of the liquid was supplied through the central orifice of the insert (2). Gas–liquid flow entered the test section (4). The design of the mixer was similar to that used by Valukina et al. (1979) for upward bubbly flow. This mixer allowed the change of the mean size of gas bubbles independent of the flow conditions.

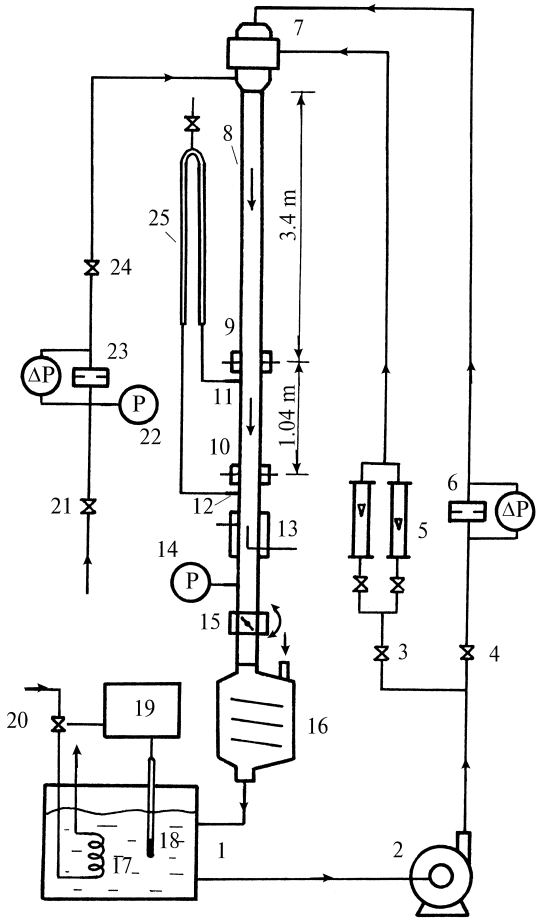

Fig. 1. Experimental set-up.

The gas flow rate ratio was determined as:

$$\beta = V_G/(V_L + V_G),$$

where V_L, V_G are superficial liquid and gas velocities, respectively. V_G was taken at the static pressure in the measuring section obtained by the manometer ((14), Fig. 1).

2.2. Measuring technique

To measure local flow parameters, an electrochemical method was used (Nakoryakov et al., 1981; 1986a). The solution of 0.005 N potassium ferri- and ferrocyanide and 0.25 M sodium carbonate in distilled water was used as the test liquid. The addition of these chemicals allowed rapid electrochemical reactions on the electrodes necessary to make flow measurements. Wall shear stress probes were thin platinum foils cemented into the test wall and polished flush with

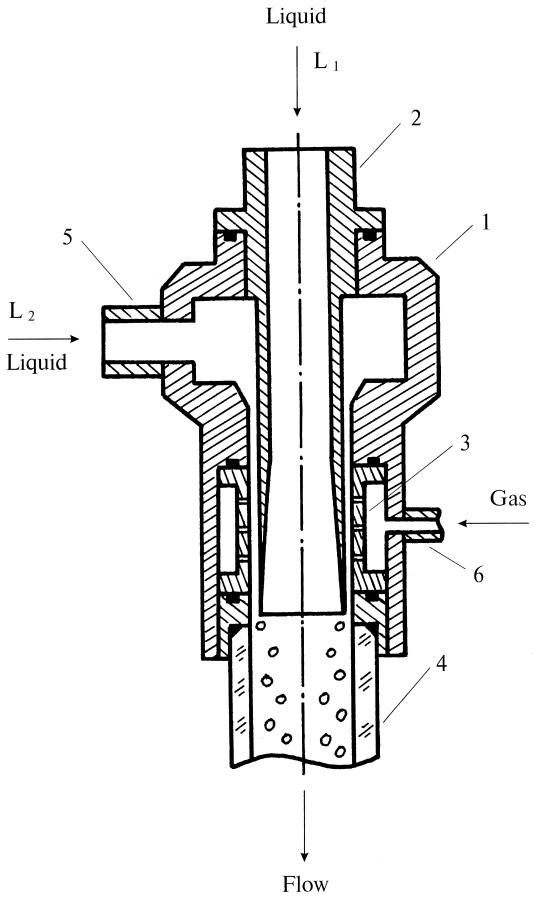

Fig. 2. Gas–liquid mixer.

it. Probes with the size of the sensitive element exposed to the flow of 0.1×0.9 mm and 0.03×0.2 mm were used for mean and fluctuating values, respectively. The probes were mounted in two measuring units ((9) and (10), Fig. 1) each containing 8 probes distributed uniformly over the pipe circumference. The probes were connected to an 8-channel D.C. amplifier converting the probe currents into the voltage. The output voltage of the amplifiers was digitized by an 8-channel A–D transformer and then processed numerically by the computer.

In order to measure liquid velocity and local void fraction a "blunt-nose" velocity probe was used (Nakoryakov et al., 1981; 1984). It was mounted in measuring unit (13) (Fig. 1). The probe was a thin platinum wire welded into a conical glass capillary. The total diameter of the probe at the measuring tip was about 50 μm. The probe signal was amplified and digitized. After that, it was processed by the computer. In order to discriminate liquid and gas phases in the probe signal, a special technique was used (Nakoryakov et al., 1984) combining electrochemical method with that of electrical conductivity.

The velocity probe was mounted on a traverse mechanism with an accuracy of positioning of 0.01 mm. The zero reading of the probe distance from the wall was measured by a microscope with the same accuracy.

Calibrations of wall shear stress and velocity probes were made in single-phase, fully developed turbulent pipe flow. The velocity probe was placed at the pipe centre during the calibration. The calibrations were made in a wide range of mean liquid velocities from 0.1 to 1.5 m/s to avoid the extrapolation of the calibration curves during measurements. The results of wall shear stress probe calibrations were plotted in the form:

$$\tau_k = A_k \cdot I_k^{C_k}$$

where τ is wall shear stress, I is the probe current, A, C are calibration coefficients, k is the number of the probe. The corresponding calibration for the velocity probe was

$$I = A_u + B_u \cdot u^{1/2},$$

where u is liquid velocity, A_u, B_u are calibration coefficients for the velocity probe.

The calibration of all the probes was made just before each two-phase experiment and repeated immediately after the experiment. The difference in the probe current between these two calibrations for the same liquid velocity did not exceed 1%.

2.3. Measurement uncertainty

The uncertainty was estimated using the r.m.s. method (Kline, 1985). Liquid and gas orifice meters were calibrated against standard devices that established the precision uncertainty interval for the liquid and gas flow rates of 1% and 2.5%, respectively. Measuring equipment used for probe current measurements provided the accuracy of current of at least 0.5%. This establishes a precision uncertainty interval for the wall shear stress of 7% and velocity measurements of 4% at a probability level of 0.95 and negligible bias since we have calibrated the probes.

Local void fraction was determined from the measurements of the time of probe residence in the gas phase. The random uncertainty of time interval measurements was less than 0.1% so it could be neglected. The bias error of void fraction measurements was caused by the process of the probe interaction with the gas bubbles. To check the accuracy of local void fraction measurements, integrated values of local void fraction were compared to the liquid holdup ϕ obtained from pressure drop and wall shear stress measurements. From this, the bias uncertainty of the local void fraction was estimated as 20%.

The error of liquid fluctuation measurements consisted of the random error and bias error. The estimate of the random error was made from the scatter of measurements; it was about 10%. The bias error resulted from the effect of transverse velocity fluctuations in the probe readings. The estimate of the bias error for the value of turbulence intensity measured in the experiments was 12%. So the total uncertainty of r.m.s. liquid velocity fluctuation measurements was 16%. Similar considerations gave the uncertainty of r.m.s. wall shear stress fluctuation measurements of 15%.

3. Experimental results and analysis

3.1. General structure of the flow

The parameters of the two-phase downward flow were measured at liquid flow rates corresponding to superficial liquid velocities $V_L = 0.5$, 0.75, 1.0 and 1.25 m/s. The values of superficial gas velocity V_G varied from 0.01 to 0.095 m/s. Experiments were made with different values of mean bubble diameter d_B. In all flow regimes, the concurrent downward bubbly flow was realized. Visual observations of the flow showed that the bubbles were pushed away from the wall, so the layer of liquid free from bubbles existed near the pipe wall. If the superficial liquid velocity was reduced below 0.5 m/s then the regime of "gas hanging" could be observed. This regime was studied in detail by Ganchev et al. (1984). It is characterized by non-zero gas holdup at zero gas flow rate. So this regime is opposite to gas-lift. The regime of "gas hanging" observed in our experiments was not sufficiently stable, so it was not studied.

Measurements of local flow parameters were performed in the flow conditions shown in Table 1. Only wall shear stress measurements were made at $V_L = 1.25$ m/s. Void fraction and velocity profiles were measured for $V_L = 0.5$–1 m/s.

An important question concerning the flow structure is the axial symmetry of the flow. In several cases, an upward bubbly flow in a vertical pipe was strongly asymmetrical, especially at low liquid velocities (Nakoryakov et al., 1986b; Kashinsky et al., 1995). Therefore, the check of

Table 1
Average flow parameters

V_L (m/s)	V_G (m/s)	β	d_b (mm)	V_m (m/s)	τ_w (N/m^2)	α_m	ϕ
1	0	0	0	1.01	2.88	0	0
0.75	0	0	0	0.752	1.74	0	0
0.5	0	0	0	0.487	0.87	0	0
1	0.0403	0.0387	1.71	1.0	3.29	0.0456	0.0403
0.75	0.03	0.0384	1.73	0.768	2.13	0.0425	0.0455
1	0.0198	0.0194	1.73	0.996	2.95	0.0235	0.0206
0.75	0.0197	0.0256	1.73	0.752	1.93	0.0293	0.0283
0.5	0.02	0.0384	1.73	0.551	1.3	0.0398	0.0498
1	0.0414	0.0398	1.46	1.02	3.24	0.0478	0.0395
0.75	0.0412	0.0521	1.46	0.78	2.24	0.0574	0.0576
0.5	0.0405	0.075	1.46	0.569	1.55	0.0882	0.0887
1	0.0916	0.0839	1.47	1.01	3.97	0.108	0.0854
0.75	0.0916	0.109	1.47	0.787	2.83	0.134	0.1165
0.5	0.0916	0.155	1.47	0.558	2.15	0.17	0.1705
1	0.019	0.0186	0.8	0.986	3	0.0221	0.0179
0.75	0.0188	0.0245	0.8	0.761	1.79	0.0289	0.0249
0.5	0.0194	0.0374	0.8	0.505	1	0.0383	0.0425
0.75	0.0407	0.0515	0.92	0.745	2.09	0.0643	0.0541
0.5	0.0418	0.0772	0.92	0.547	1.35	0.0736	0.0877
1	0.0918	0.0841	0.96	0.979	3.83	0.104	0.0829
0.75	0.0942	0.1116	0.96	0.791	2.83	0.13	0.1155
0.5	0.0924	0.156	0.96	0.576	1.98	0.162	0.1591

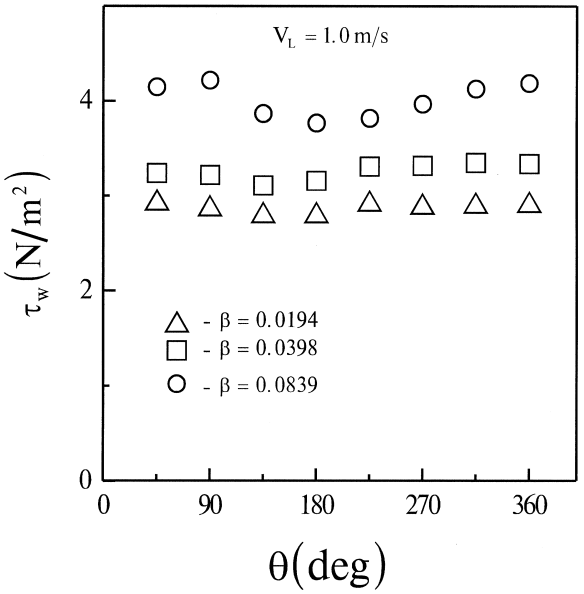

Fig. 3. Circumferential distribution of wall shear stress, $V_L = 1.0$ m/s.

axial symmetry was made in the downward flow. Figs. 3 and 4 show typical distributions of local wall shear stress $\tau_W(\theta)$ measured in the same pipe cross section at different circumferential positions. Here, θ is a circumferential angle counted from the position of the first wall shear stress probe. The deviation of local τ_W values around the mean value for the same flow

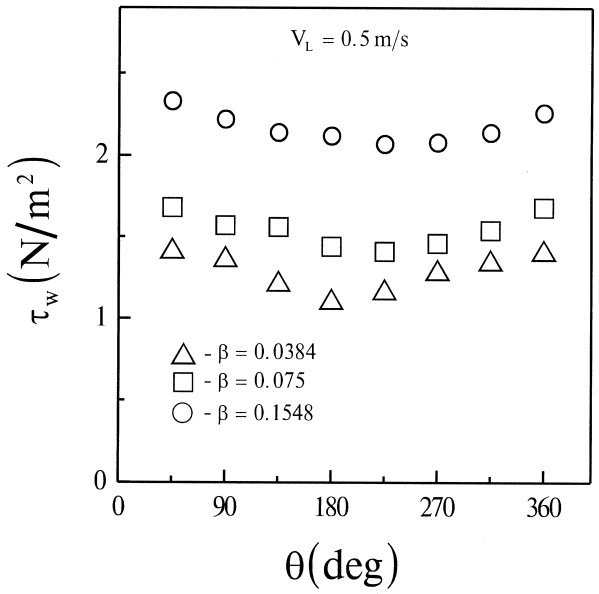

Fig. 4. Circumferential distribution of wall shear stress, $V_L = 0.5$ m/s.

conditions did not exceed 10% at superficial liquid velocities $V_L > 0.75$ m/s. At the smallest V_L the deviation was less than 20%. So in all cases, downward bubbly flow may be considered as axisymmetrical.

3.2. Wall shear stress

Mean cross-sectional wall shear stress τ_W was obtained by averaging the readings of all 8 probes. Results of the measurements are presented in Fig. 5 as the ratio τ_W/τ_0 vs gas flow rate ratio β. Here, τ_0 is wall shear stress in a single-phase turbulent flow with the same superficial liquid velocity V_L. Results for different V_L and two bubble diameters are shown.

In all flow regimes, the ratio $\tau_W/\tau_0 > 1$, so the two-phase wall shear stress in downward flow is always higher than the single-phase one. The same trend was observed in upward bubbly flow in a vertical pipe (Nakoryakov et al., 1981). A direct measurement of two-phase wall shear stress in downward flow was made before by Gorelik et al. (1987) for a 15 mm diameter pipe. A similar increase of wall shear stress as compared to single-phase values was observed. The ratio τ_W/τ_0 in the present experiments is higher than that given by Armand (1946) correlation:

$$\tau_W/\tau_0 = (1 - 0.833\beta)^{-1.53}. \tag{1}$$

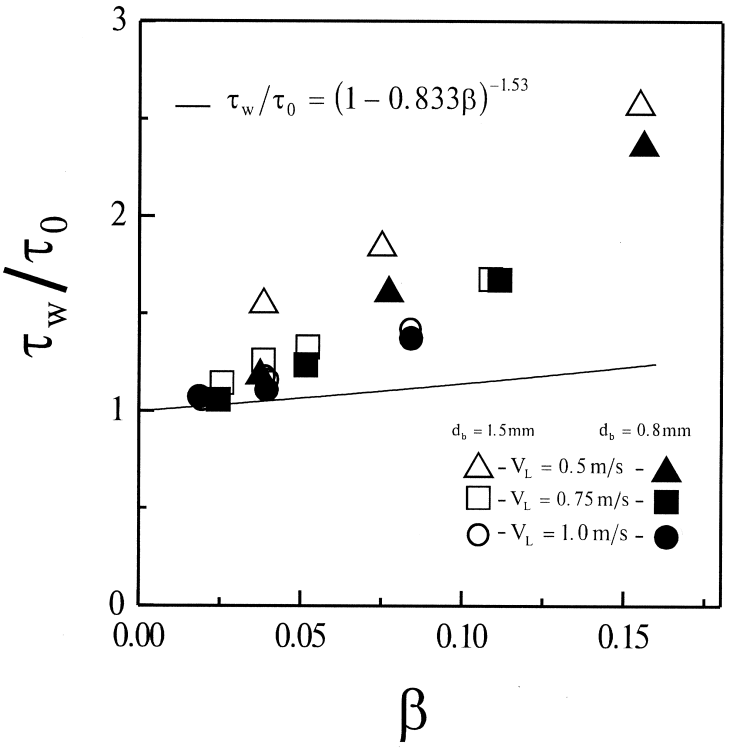

Fig. 5. Mean wall shear stress.

This correlation is also shown in Fig. 5. It is interesting to note that the size of gas bubbles produces a significant effect on the wall shear stress. The value of τ_W increases with increasing bubble size.

The prediction of wall shear stress in a downward bubbly flow was made by Clark and Flemmer (1985a). On the basis of mixing length theory a simple formula for wall shear stress calculation was suggested:

$$\tau_C/\tau_0 = (1-\varepsilon)^{-1}\left[(1-\varepsilon)^{-1} + BU_B\varepsilon/V_L\right]. \tag{2}$$

Here, τ_C is calculated wall shear stress, ε is calculated gas holdup:

$$\varepsilon = \beta/\left(1 + U_B(1-\beta)/V_L\right), \tag{3}$$

U_B is the terminal speed of gas bubbles in a stagnant liquid. The empirical coefficient B was chosen as 22.81 for downflow (Clark and Flemmer, 1985a).

The comparison of the experimental data with (2) was made. The values of U_B were obtained from measured d_B using the correlation of Wallis (1974) for tap water. The results of this comparison are shown in Fig. 6. The agreement of measured and calculated wall shear stress values is reasonably good, the discrepancy does not exceed $\pm$15 %.

An important question concerning two-phase flow is the flow stabilization along the pipe. To check it, simultaneous measurements of wall shear stress in two sections of the pipe were performed. This was done using two measuring units ((9) and (10) in Fig. 1). The comparison of τ_W values for both sections is shown in Fig. 7. The results agree to the accuracy of 5% which is in the limits of measurement uncertainty. So the flow may be regarded as stabilized for all liquid and gas flow rates.

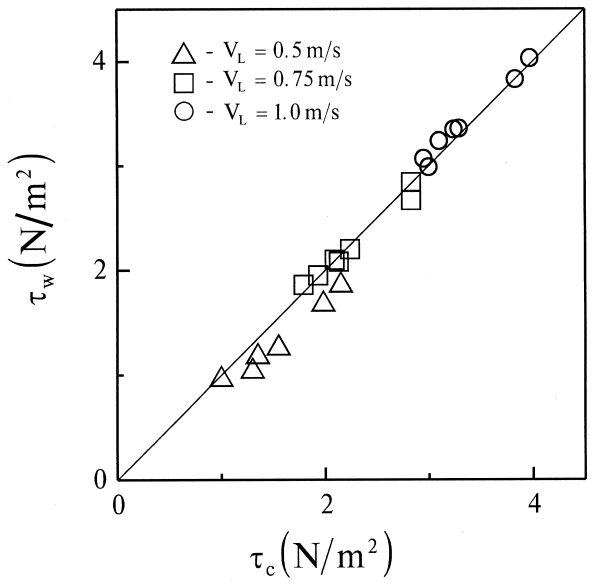

Fig. 6. Comparison with the prediction of Clark and Flemmer (1985a).

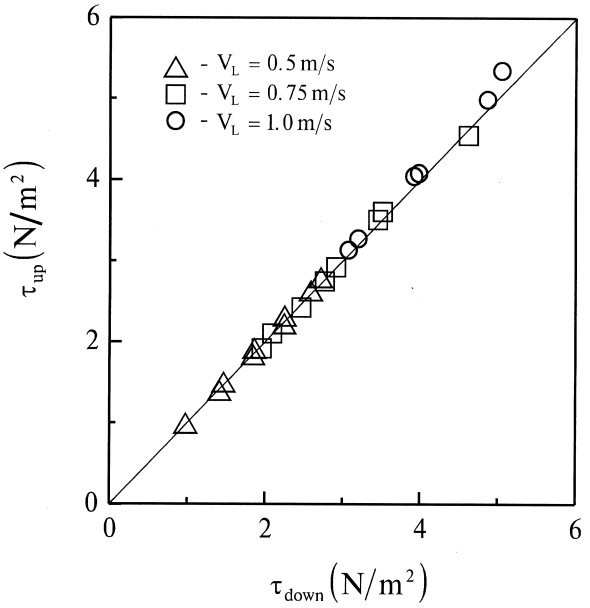

Fig. 7. Wall shear stress stabilization along the pipe.

3.3. Void fraction measurements

Local void fraction profiles were measured for different values of liquid and gas flow rates. The profiles of α are shown in Figs. 8–10 for superficial liquid velocities $V_L = 0.5$, 0.75 and

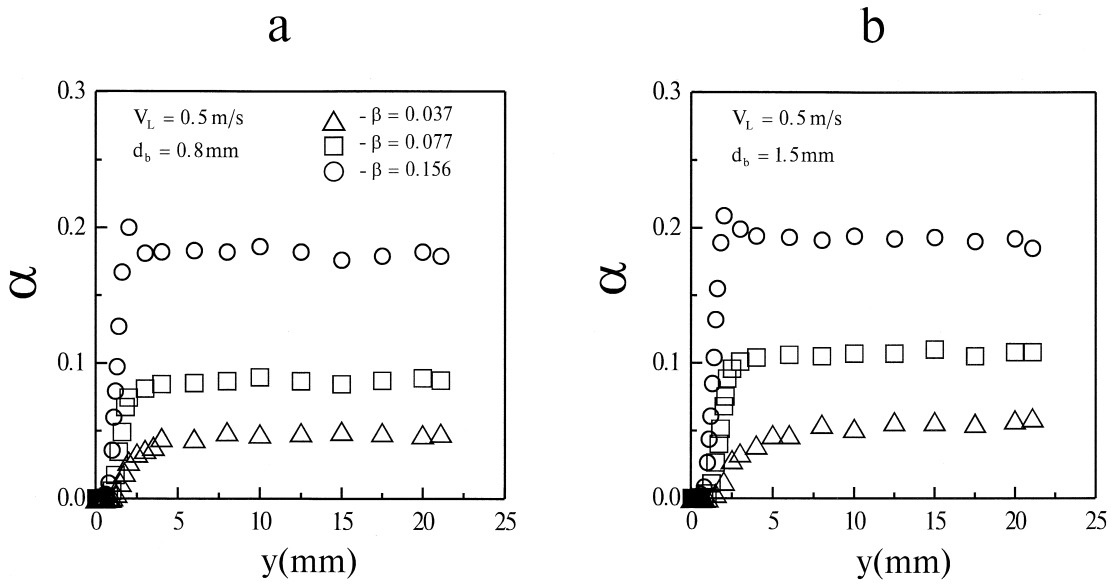

Fig. 8. Local void fraction, $V_L = 0.5$ m/s.

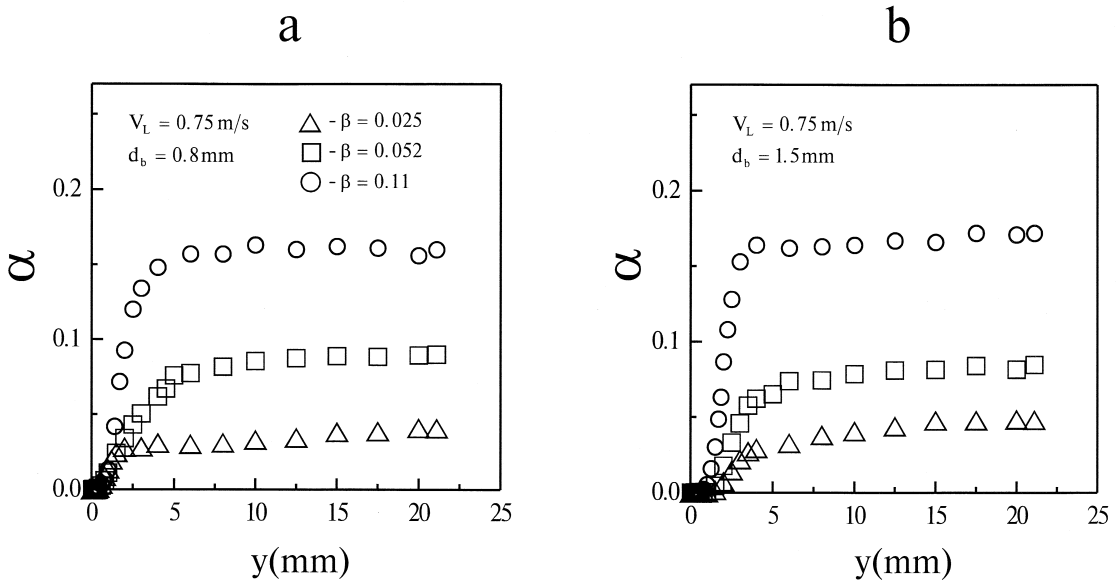

Fig. 9. Local void fraction, $V_L = 0.75$ m/s.

1.0 m/s, respectively, with y being the distance from the wall. Data for two different bubble sizes are presented. All void profiles have zero value of α close to the wall, and rather uniform distribution in the central part of the pipe. The region of α increase from zero to the central value is closer to the wall at lower liquid velocity. The effect of bubble size on void distribution

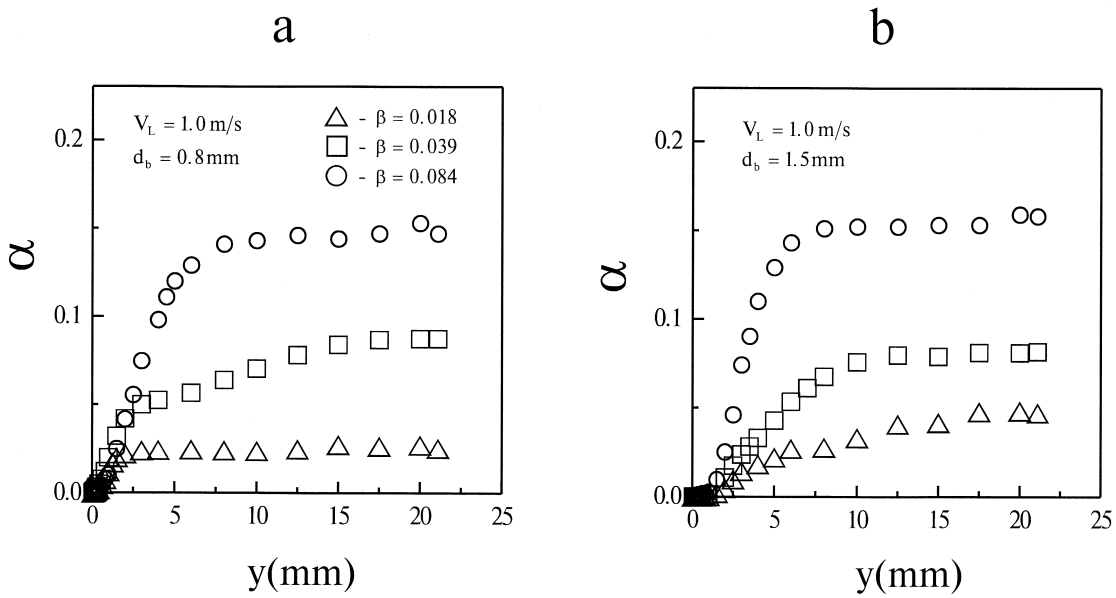

Fig. 10. Local void fraction, $V_L = 1.0$ m/s.

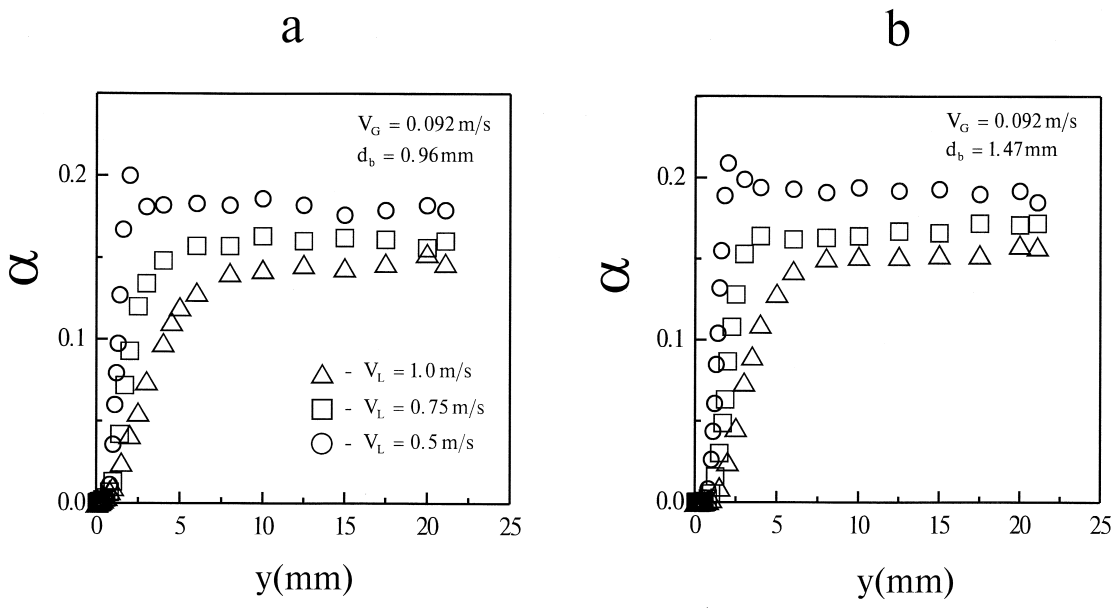

Fig. 11. Effect of liquid velocity on local void fraction.

is not too pronounced in these figures. The effect of liquid velocity on α profiles is clearly seen in Fig. 11 where data for the same superficial gas velocity V_G and different liquid velocities are shown. At lower V_L the bubbles come closer to the wall. Generally, the effect of bubble size is less than the effect of liquid velocity.

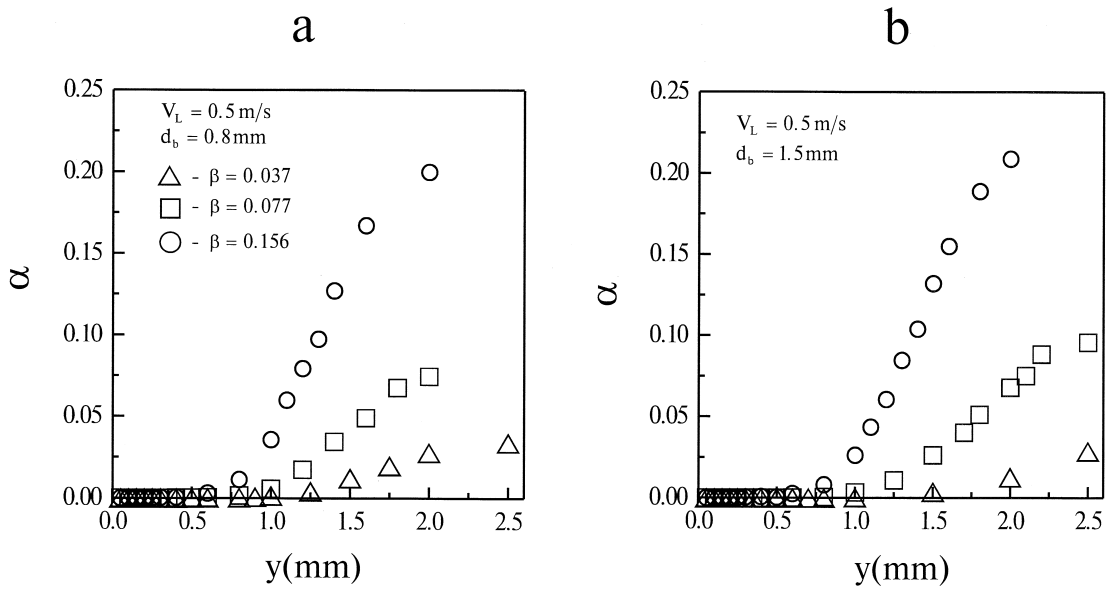

Fig. 12. Local void fraction close to the wall, V_L = 0.5 m/s.

Some of the profiles at $V_L = 0.5$ m/s and high values of β have small local maxima of α close to the wall. This effect was noted for low-velocity downward flows also by Ganchev et al. (1984).

Typical distributions of local void fraction close to the wall are shown in Figs. 12–13. $\alpha(y)$ is zero up to some distance from the wall. This distance depends on the flow parameters. The effect of bubble size on near-wall void distribution is small for $V_L = 0.5$ m/s but becomes pronounced at $V_L = 1$ m/s. Smaller bubbles come closer to the wall, so the region of zero void fraction is not so distinct in Fig. 13(a).

Average values of void fraction α_m were calculated from local distributions by averaging α over the pipe cross section:

$$\alpha_m = \frac{2}{R^2}\int_0^R \alpha(r) r \, dr. \tag{4}$$

Here, R is pipe radius. The values of α_m for different flow regimes are presented in Table 1. They are also shown in Fig. 14 vs gas flow rate ratio β. In almost all conditions, $\alpha_m > \beta$. This correlates with the measurements of Ganchev et al. (1984).

3.4. Liquid velocity

Measured profiles of liquid velocity u are shown in Figs. 15–17. Here, u_1 is liquid velocity in the pipe center. Velocity distributions for single-phase flow are also presented (profiles with $\beta = 0$). In all flow regimes two-phase profiles are more filled compared to single-phase ones. This behavior is qualitatively the same as in upward bubbly flow (Serizawa et al., 1975; Nakoryakov et al., 1981). Some effect of bubble size can be observed: the deformation of

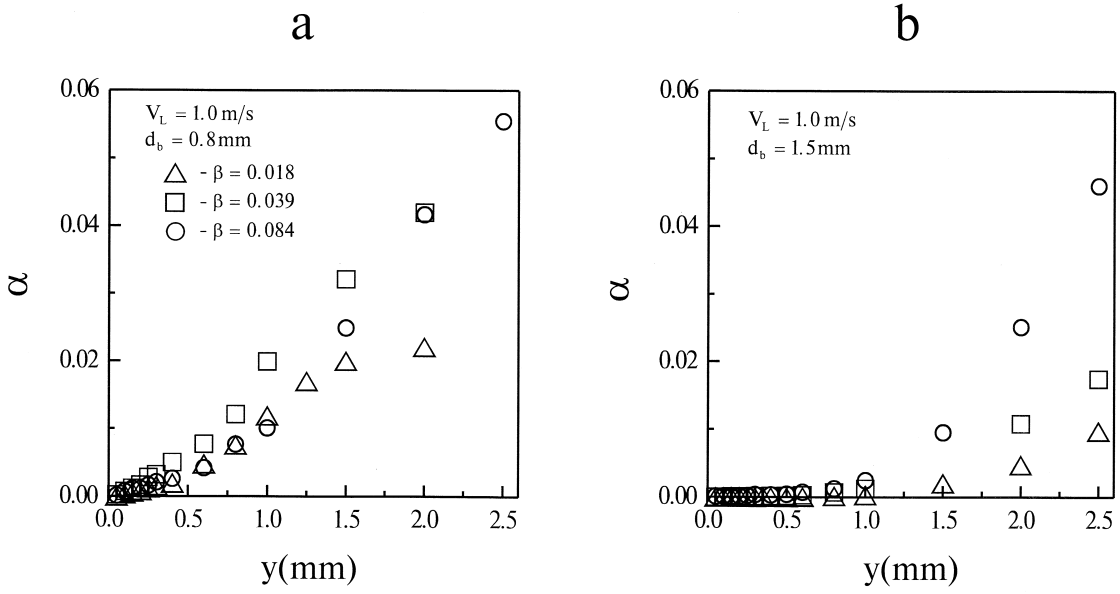

Fig. 13. Local void fraction close to the wall, $V_L = 1.0$ m/s.

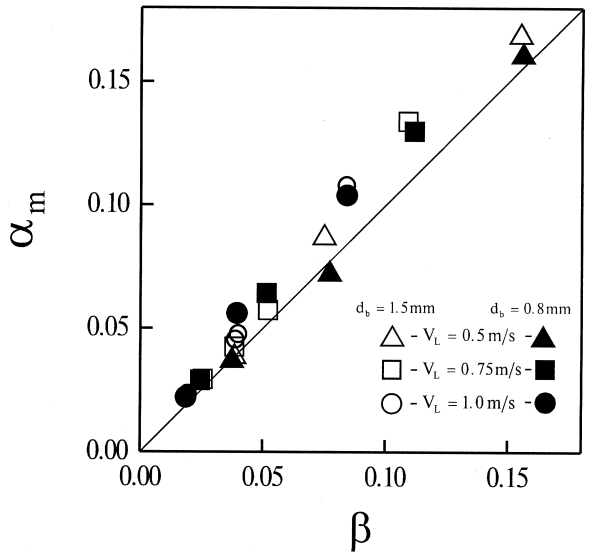

Fig. 14. Mean cross-sectional void fraction.

velocity becomes more for larger bubbles. Again, the most significant parameters affecting the velocity distribution are superficial liquid velocity and gas flow rate ratio. At $V_L = 0.5$ m/s and highest β values, the liquid velocity profile is completely flattened in the central part of the pipe. Small local velocity maxima exist near the wall. Similar maxima were observed by

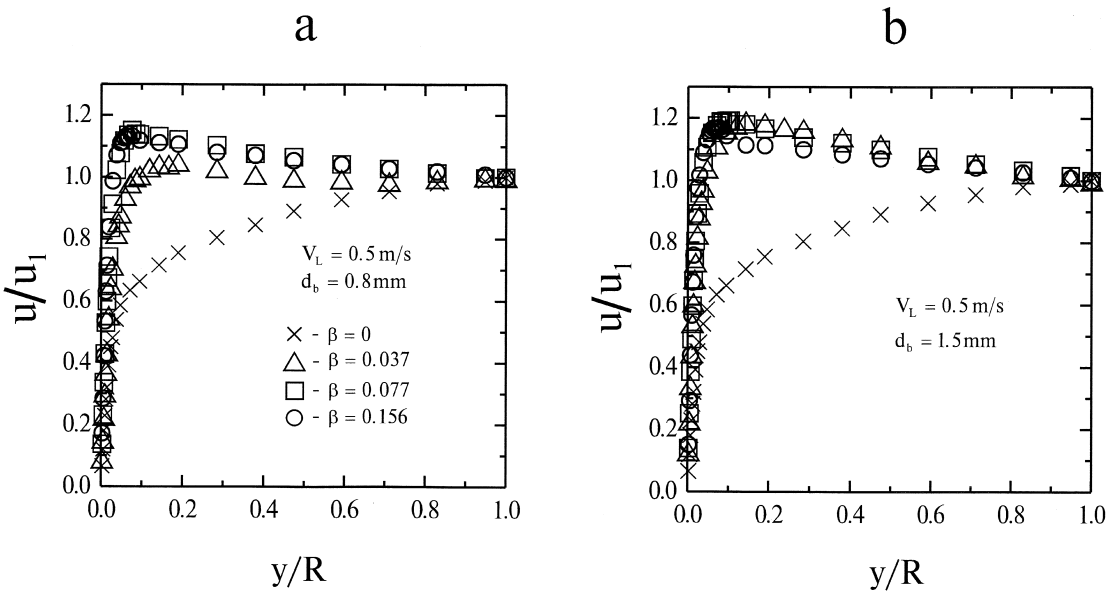

Fig. 15. Liquid velocity, $V_L = 0.5$ m/s.

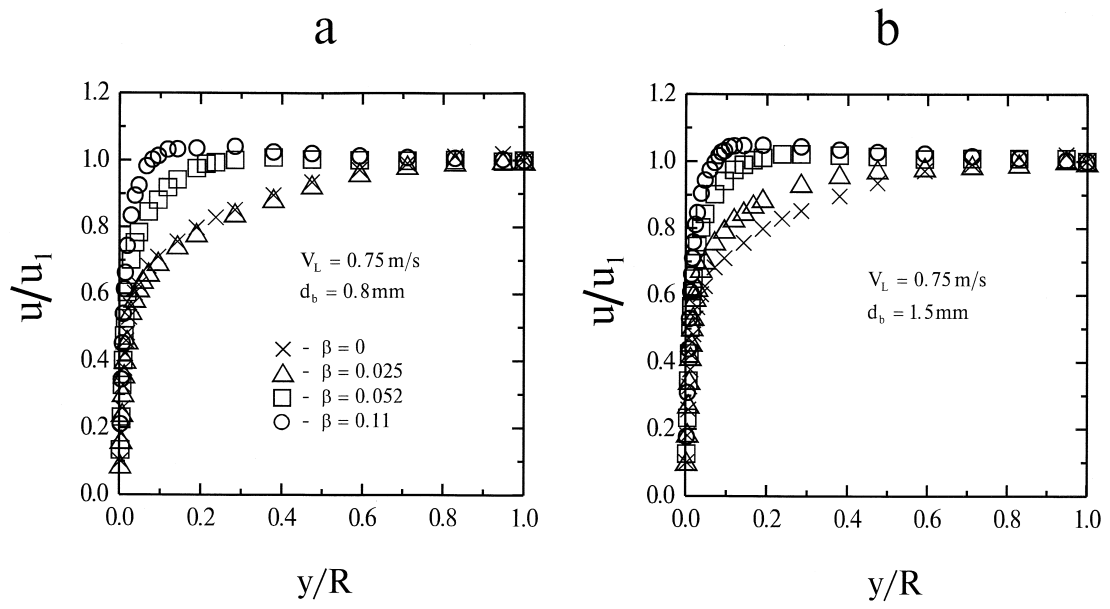

Fig. 16. Liquid velocity, $V_L = 0.75$ m/s.

Ganchev and Peresadko (1985) and Wang et al. (1987). The increase of gas flow rate ratio results in a higher velocity gradient near the wall, hence in higher wall shear stress (Fig. 5).

The effect of superficial liquid velocity on the shape of velocity distribution is clearly demonstrated in Fig. 18, where data for different V_L and the same β and d_B are shown.

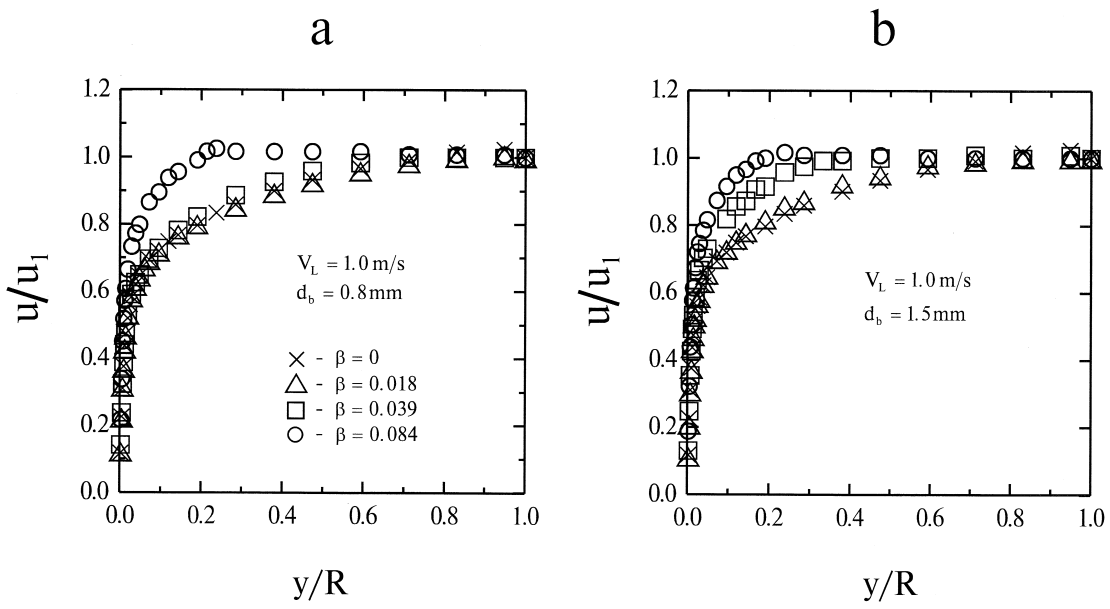

Fig. 17. Liquid velocity, $V_L = 1.0$ m/s

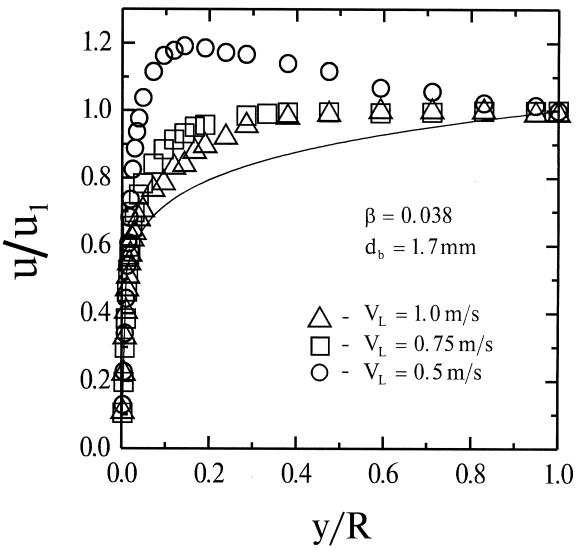

Fig. 18. Effect of superficial liquid velocity on velocity profiles.

Mean cross-sectional liquid velocity V_m was calculated from the velocity profiles:

$$V_m = \frac{2}{R^2}\int_0^R ru(r)(1-\alpha)\,dr. \tag{5}$$

Values of V_m are presented in Table 1. The deviation of V_m from superficial liquid velocity V_L did not exceed 5.5% for $V_L = 0.75$ and 1 m/s. It is close to the value of measurement uncertainty for the velocity. For $V_L = 0.5$ m/s, the discrepancy of V_m and V_L were higher, from 9% to 15% at the highest β values. This difference, which is out of the estimated measurement uncertainty, may be attributed to a slight flow asymmetry which existed and was higher at low liquid velocity (see Fig. 4). The difference is in the limits of the wall shear stress variation around the mean value.

3.5. Near-wall velocity distribution

Liquid velocity profiles were plotted in the wall coordinates u/u_τ vs yu_τ/v. Here, friction velocity $u_\tau = (\tau_W/\rho)^{1/2}$, where τ_W is measured two-phase wall shear stress, ρ, v are liquid density and viscosity. Results are presented in Figs. 19–21. Solid lines on the figures show the corresponding single-phase distributions for viscous sublayer and turbulent core (Schlichting, 1969). Results agree fairly well with single-phase correlations. At $V_L \geq 0.75$ m/s, the single-phase "law-of-the-wall" holds up to the value of yu_τ/v of about 200. At $V_L = 0.5$ m/s, this law is valid up to $yu_\tau/v = 50$ to 70. At higher distances from the wall, the deviation from the single-phase distribution is caused by the flattening of the velocity profile.

Measurements of liquid velocity in upward bubbly flow (Moursali et al., 1995; Nakoryakov and Kashinsky, 1995) demonstrated a significant deviation of two-phase profiles from the single-phase correlation. This was attributed to the existence of the near-wall void peak in

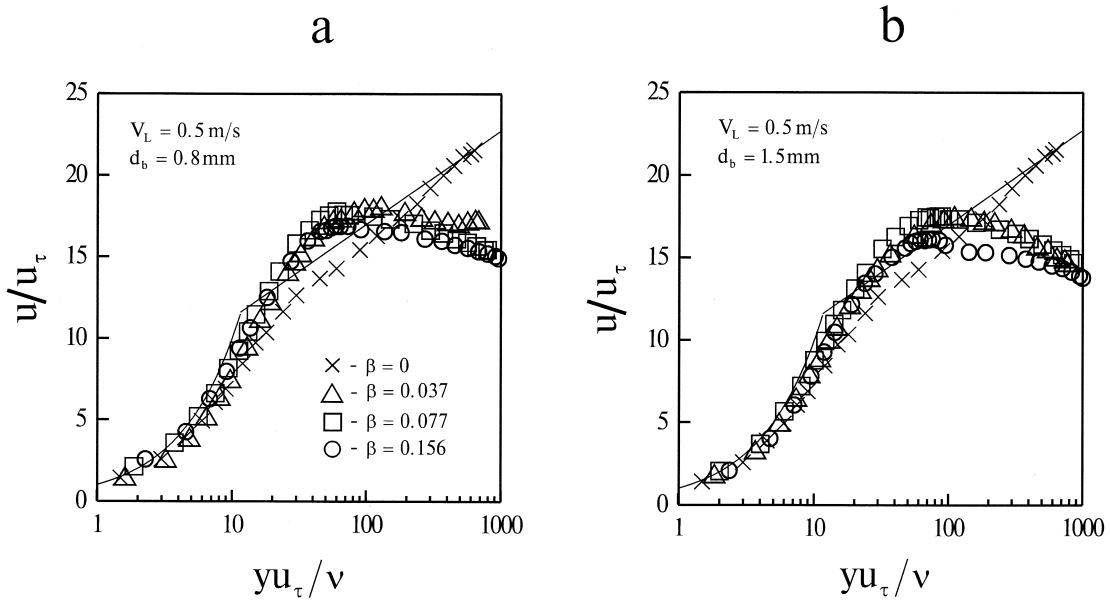

Fig. 19. Liquid velocity in the wall coordinates, $V_L = 0.5$ m/s.

upward flow. In contrast, in downward bubbly flow, no bubbles come close to the wall. Therefore the near-wall region of the flow obeys the single-phase law to a good accuracy. The conservation of the "law-of-the-wall" in gas–liquid flow is an important assumption used in the theoretical models to describe the flow near the wall (see, e.g. Marie, 1987).

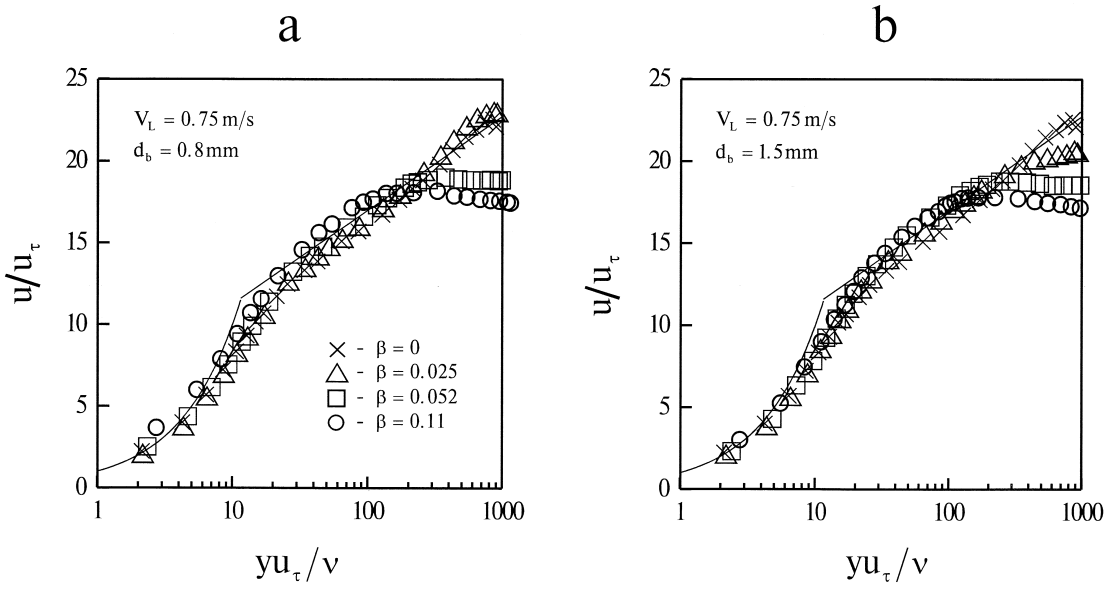

Fig. 20. Liquid velocity in the wall coordinates, $V_L = 0.75$ m/s.

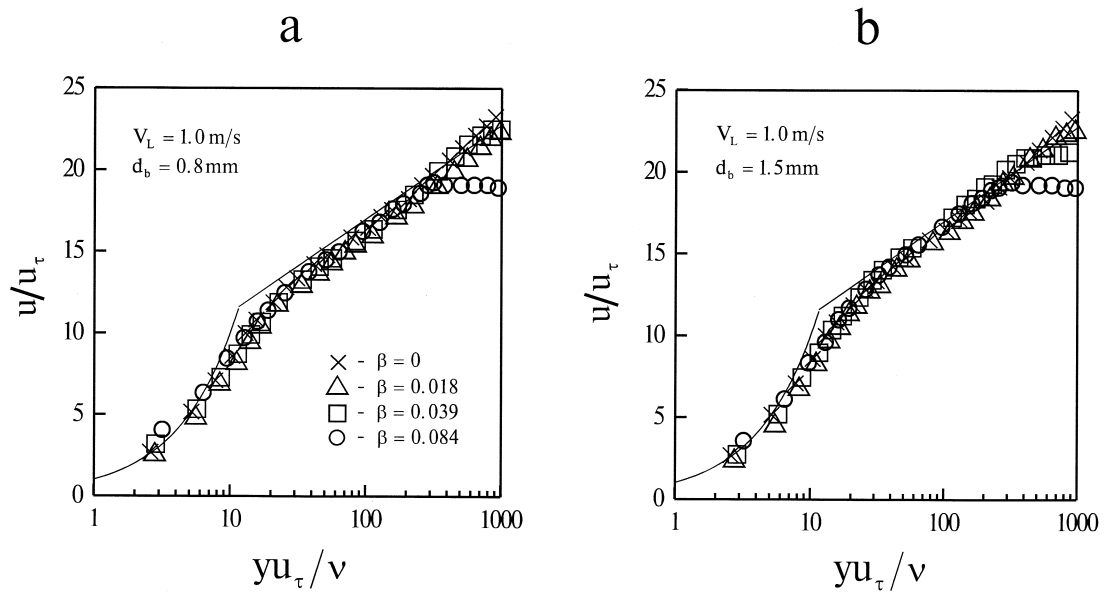

Fig. 21. Liquid velocity in the wall coordinates, $V_L = 1.0$ m/s.

A presentation of void profiles in the wall coordinates is shown in Figs 22-23. The region of zero void fraction extends up to $yu_\tau/\nu = 50$ at $V_L = 0.5$ m/s and up to $yu_\tau/\nu = 100$ at $V_L = 1.0$ m/s for a bubble diameter of 1.5 mm. The effect of bubble size on the void

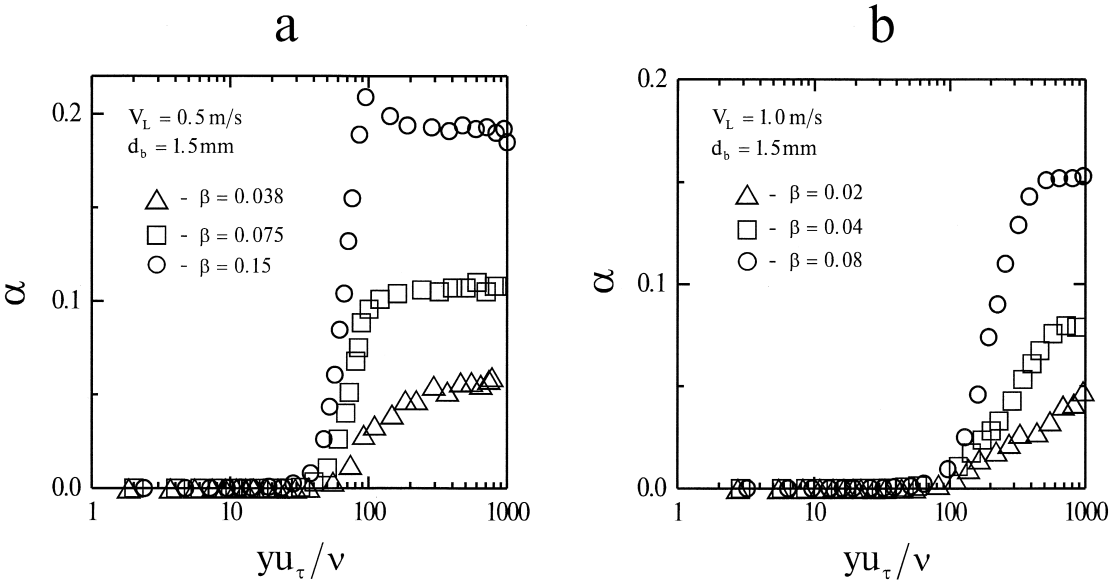

Fig. 22. Local void fraction in the wall coordinates.

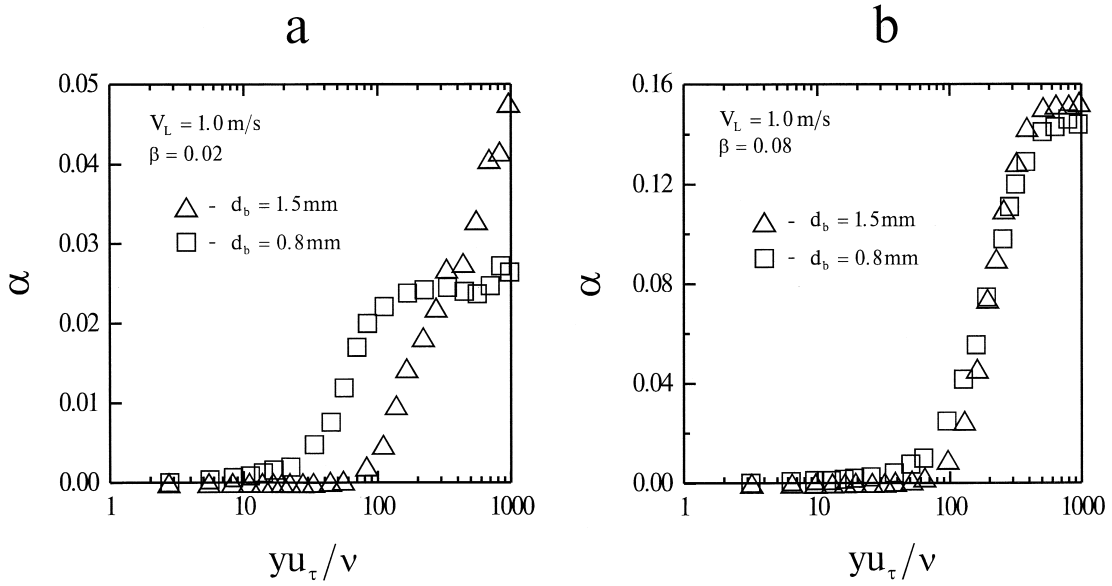

Fig. 23. Effect of bubble size in void distribution.

distribution is evident at $V_L = 1.0$ m/s and $\beta = 0.02$ (Fig. 23). At higher values of β, this effect becomes less.

It can also be seen from the velocity distributions (Figs. 19–21) that the viscous sublayer exists in downward bubbly flow up to the dimensionless distance from the wall of at least 10. Again, it was not the case in upward flows with a pronounced wall void peak (Nakoryakov and Kashinsky, 1995). Results presented show that actual wall shear stress (or friction velocity) in a downward bubbly flow is an appropriate parameter describing the near-wall region of the flow. No "effective" wall shear stress is needed as it was done by Marie et al. (1997) for upward bubbly flow along a flat plate.

3.6. Wall shear stress and velocity fluctuations

The presence of the gas phase usually changes the fluctuational structure of the flow (Serizawa et al., 1975; Michiyoshi and Serizawa, 1986). An important parameter characterizing the flow fluctuations close to the wall is the relative intensity of wall shear stress fluctuations τ'_W/τ_W, where τ'_W is r.m.s. intensity of wall shear stress fluctuations. In a single-phase turbulent pipe flow, the value of τ'_W/τ_W is approximately the same, equal to 0.37–0.38. Measurements in upward bubbly flow (Nakoryakov et al., 1981) have demonstrated an increase in τ'_W/τ_W compared to a single-phase flow. Results of downward flow experiments are presented in Fig. 24. At $V_L = 1$ m/s, the intensity of the fluctuations τ'_W/τ_W remains approximately the same as in the single-phase flow ($\beta = 0$). At lower liquid velocities, a decrease of τ'_W/τ_W is observed. It is especially evident at $V_L = 0.5$ m/s, the values of τ'_W/τ_W fall up to 0.23–0.25. This result demonstrates the existence of turbulence suppression mechanisms in downward flow. Although the relative fluctuation τ'_W/τ_W is less than in single-phase flow, the dimensional τ'_W values are

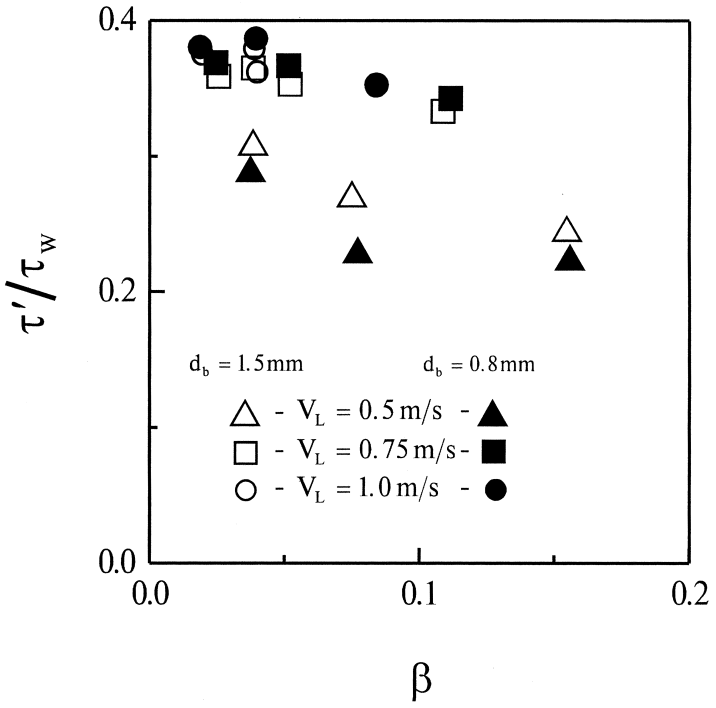

Fig. 24. Wall shear stress fluctuations.

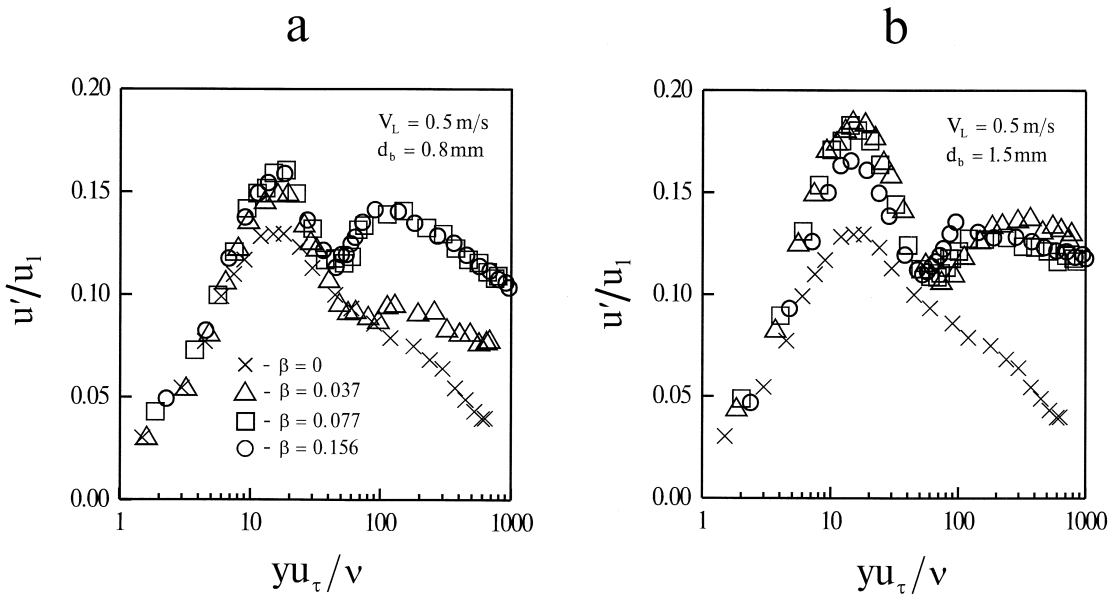

Fig. 25. Liquid velocity fluctuations, $V_L = 0.5$ m/s.

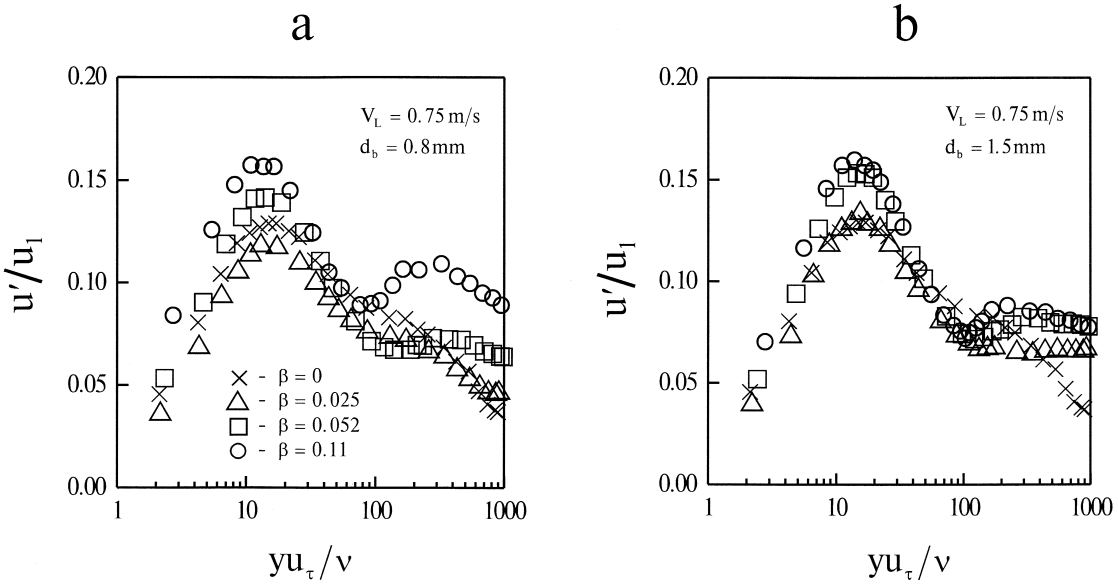

Fig. 26. Liquid velocity fluctuations, $V_L = 0.75$ m/s.

either equal to or greater than those in single-phase flow because the mean wall shear stress also increases.

Relative intensity of liquid velocity fluctuations u'/u_1 is plotted in Figs 25–27. Here, u' is r.m.s. liquid velocity fluctuation, u_1 is liquid velocity in the pipe centre. Different behavior of

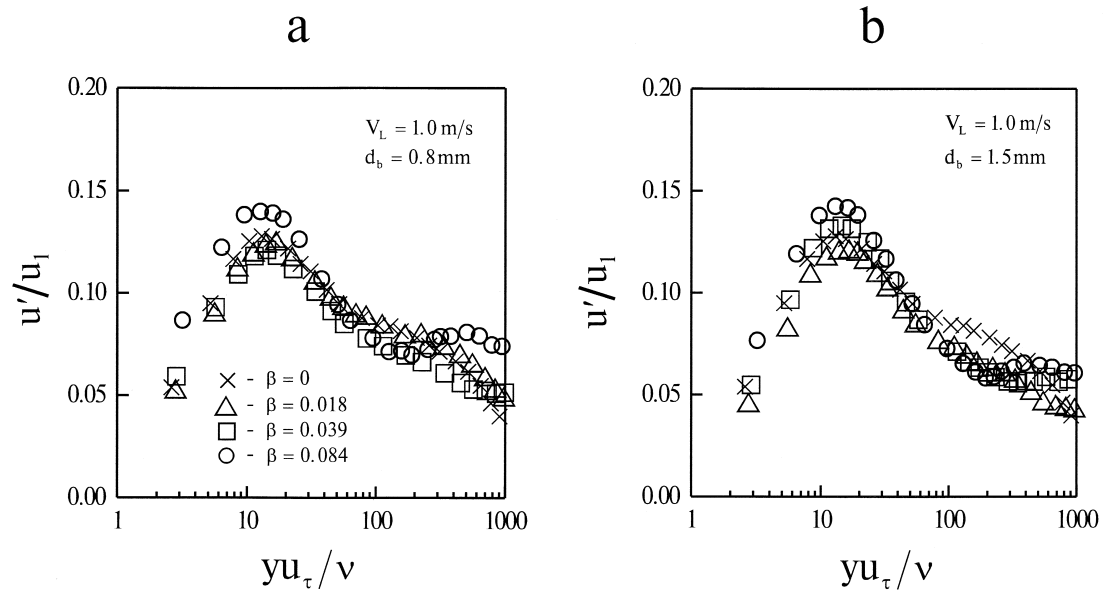

Fig. 27. Liquid velocity fluctuations, $V_L = 1.0$ m/s.

fluctuations is observed in various regions of the flow. In the central part of the pipe, two-phase values of u'/u_1 are higher than in single-phase flow (profiles with $\beta = 0$), particularly at $V_L = 0.5$ m/s. This is the result of liquid agitation by bubbles moving with a definite relative velocity. Close to the wall, the values of u'/u_1 may be either higher or lower than in single-phase flow. Similar result were obtained in downward flow by Wang et al. (1987).

Figs. 28–30 show liquid velocity fluctuations normalized by friction velocity u_τ instead of u_1. This presentation is more adequate for the near-wall region of the flow. In these coordinates, single-phase and two-phase velocity fluctuations correlate well just near the wall in the viscous sublayer, at $yu_\tau/\nu < 30$. For $V_L = 0.5$ m/s the two-phase fluctuations are slightly smaller than in single-phase flow even at smallest yu_τ/ν in the viscous sublayer. However, this reduction is in the limits of measurement uncertainty.

In the region of yu_τ/ν from 20 to 50–70, two-phase fluctuations are sufficiently less than in single-phase flow. However, the values of local void fraction in this region are still zero (see Figs. 22 and 23). So the damping of fluctuations takes place in the layer of bubble-free liquid adjacent to the central region of high bubble concentration.

Several profiles of liquid velocity fluctuations have two peaks, this is clear in Figs. 28 and 29. The closest to the wall peak corresponds to the wall-induced turbulence, the highest value of u'/u_τ is at $yu_\tau/\nu = 10$–30 both in single-phase and in two-phase flows. In this region, the friction velocity u_τ is the main parameter determining the fluctuation distribution. The second peak, distant from the wall, is that of bubble-induced turbulence. It starts at $yu_\tau/\nu = 70$–100. Just at these values of yu_τ/ν, the increase of α begins from zero value close to the wall (Figs. 22 and 23). In the central region of the pipe, the bubble-induced turbulence is significantly higher than in single-phase flow.

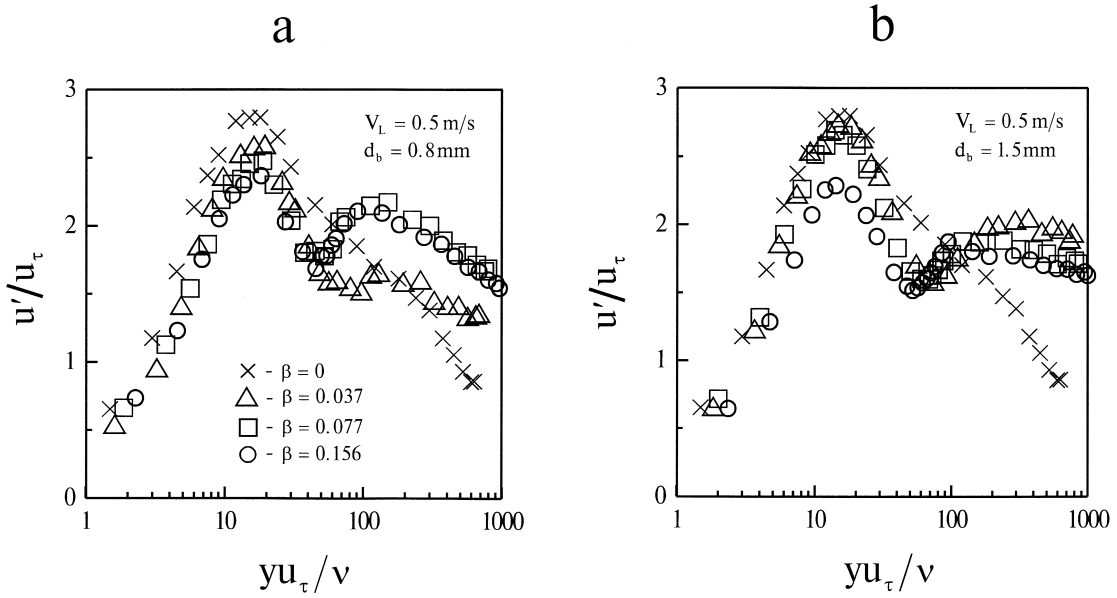

Fig. 28. Liquid velocity fluctuations in the wall coordinates, $V_L = 0.5$ m/s.

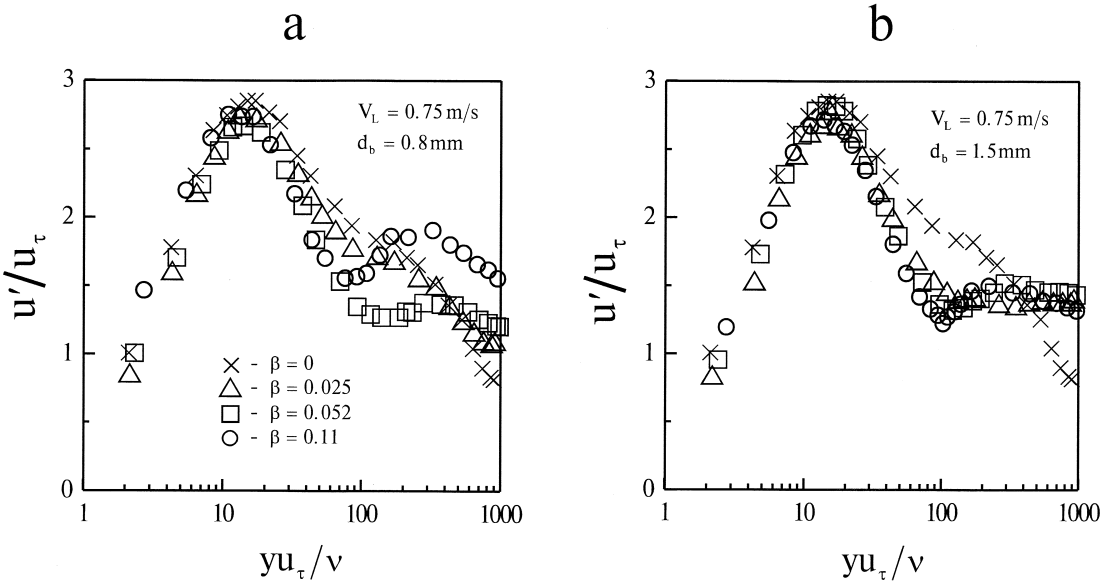

Fig. 29. Liquid velocity fluctuations in the wall coordinates, $V_L = 0.75$ m/s.

3.7. Analysis of void fraction and liquid velocity distributions

A transverse lift force acting on a bubble rising with relative velocity U_R in a flow with a liquid velocity gradient has the form (Ibragimov et al., 1973; Zun, 1980):

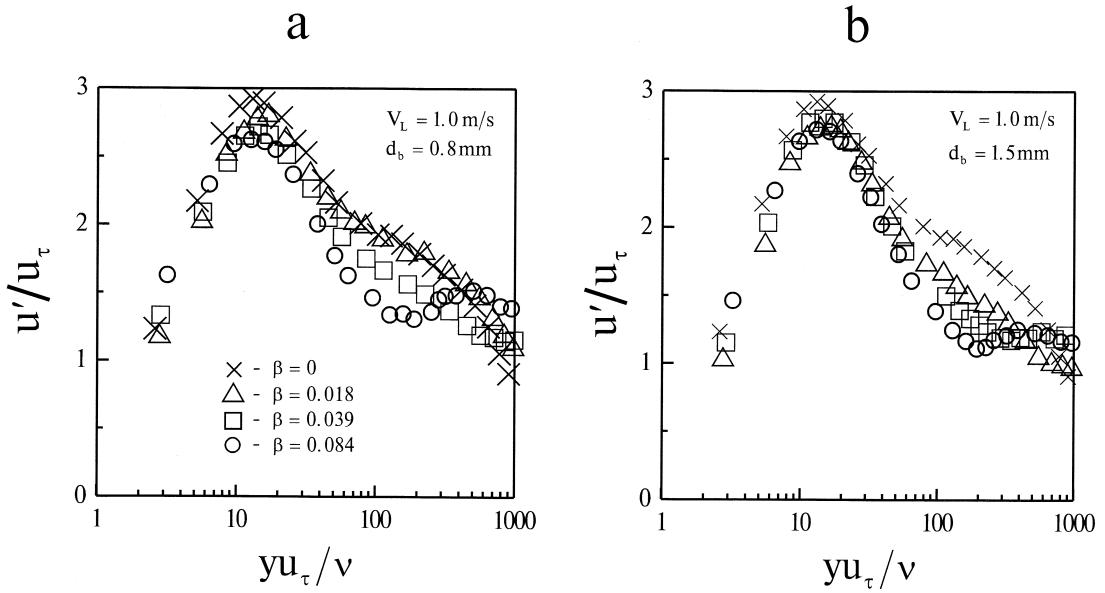

Fig. 30. Liquid velocity fluctuations in the wall coordinates, $V_L = 1.0$ m/s.

$$M_L = A_L \rho \alpha U_R \, du/dy \tag{6}$$

where U_R is the relative velocity of a bubble, the lift coefficient A_L depends significantly on the flow conditions (Wang et al., 1987). This force has opposite signs for upward and downward flows.

In the formation of void distribution a wall repulsion force may also play an important role. The expression for this force is proposed by Antal et al. (1991):

$$M_W = -\frac{\alpha \rho U_R^2}{R_B^2}\left[C_{W1} + C_{W2}(R_B/y_0)\right], \tag{7}$$

where R_B is bubble radius, y_0 is distance from the wall to the bubble centre. The coefficients in (7) are defined as:

$$C_{W1} = -0.06U_R - 0.104 \quad \text{and} \quad C_{W2} = 0.147.$$

The wall repulsion force has the same sign in upward and downward flows. It always pushes the bubbles from the wall.

Besides, the void distribution is affected by liquid turbulence. This may have less effect at low liquid velocities.

In an upward flow, the lift force pushes the bubbles towards the wall acting against the wall repulsion force. Hence, in definite flow conditions, a wall void peak is observed. Contrarily, in a downward flow, both forces push the bubble away from the wall. This produces a bubble-free region near the wall. This is the region of a strong velocity gradient in which the wall force is the highest.

Calculations of the void distribution in downward bubbly flow performed by Wang et al. (1987), Drew and Lahey (1982) and Antal et al. (1991) give a uniform distribution of α in the central part of the tube and a region of zero near the wall, at relative radius $r/R < 0.9$–0.95. This is qualitatively consistent with the present results on void fraction shown in Figs. 8–10.

The effect of the lift force on the bubble motion depends strongly on the magnitude of the liquid velocity gradient. For this reason, the bubble migration was not observed in a free shear bubbly flow where the value of the velocity gradient is sufficiently less than in near-wall flows (Lance et al., 1991).

As was shown in Section 3.4, the main feature of the velocity profiles is their flattening. This is also typical for upward bubbly flow (Nakoryakov et al., 1981).

A shear stress distribution across the pipe was calculated from the force balance using a formula similar to that of Clark et al. (1990):

$$\tau = \tau_W\left(\frac{r}{R}\right) - \frac{1}{2} rg\left[\bar{\rho} - \rho_i(r)\right] \tag{8}$$

where $\bar{\rho}$ and ρ_i is the difference between the average density over the whole radius, and the average density within a radius r.

Both $\bar{\rho}$ and ρ_i were calculated from measured $\alpha(y)$ distribution. Experimental values of τ_W were taken in (8). Results of shear stress calculation for different regimes are shown in Fig. 31. The buoyant forces result in the decrease of shear stress in the central part of the pipe. This decrease is more pronounced at low liquid velocities. Actually, at $V_L = 0.5$ m/s the value

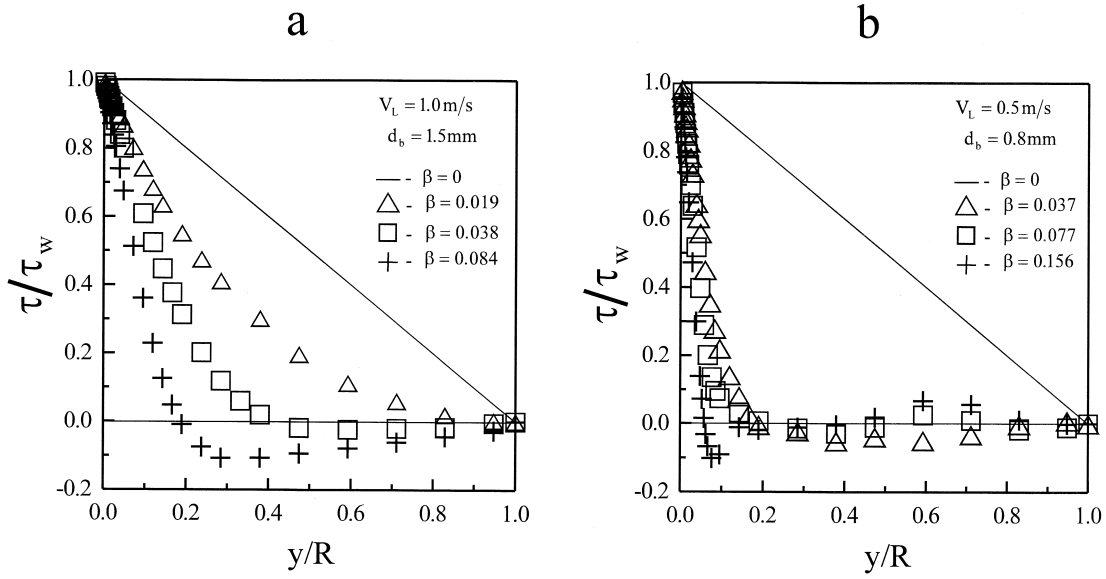

Fig. 31. Shear stress distribution across the pipe.

of τ/τ_W is close to zero at $y > 5$ mm. This means that the shear stress induced by the wall is completely compensated for by buoyant forces. Besides, negative values of τ are observed in several regimes. This deformation of the shear stress profile is the most significant factor affecting the deformation of the velocity profile compared to single-phase flow. The second important factor is the increase of the liquid turbulence in the central part of the pipe as shown by Marie (1987).

The liquid velocity profile may be calculated from $\tau(r)$ distribution using the relation (Sato et al., 1981):

$$\tau = (1-\alpha)\left(v + \varepsilon' + \varepsilon''\right) \mathrm{d}u/\mathrm{d}y \tag{9}$$

where v is liquid viscosity, ε' and ε'' are turbulent and two-phase eddy diffusivities, correspondingly.

It is clear from (9) that a decrease of τ results in a decrease of the velocity gradient, and, hence, to a liquid velocity profile flattening. In the regions where τ is negative, the slope of the velocity profile also changes its sign which can be observed for measured profiles at $V_1 = 0.5$ m/s (Fig. 15).

However, a direct application of the prediction technique of Sato et al. (1981) did not give satisfactory results in liquid velocity distributions. The technique predicted higher wall shear stress values than those obtained from the measurements. Therefore, for downward flow, the expressions for ε' and ε'' should be modified compared to Sato et al. (1981).

The flattening of the velocity profile results in the decrease of the single-phase turbulence production ($\bar{u}'\bar{v}'$ $\mathrm{d}u/\mathrm{d}y$) due to a small value of the liquid velocity gradient. It can be observed in Fig. 32, where mean liquid velocity and velocity fluctuation are shown for $V_1 = 1$ m/s, $\beta = 0.04$. The region of flattened velocity in the central part of the pipe

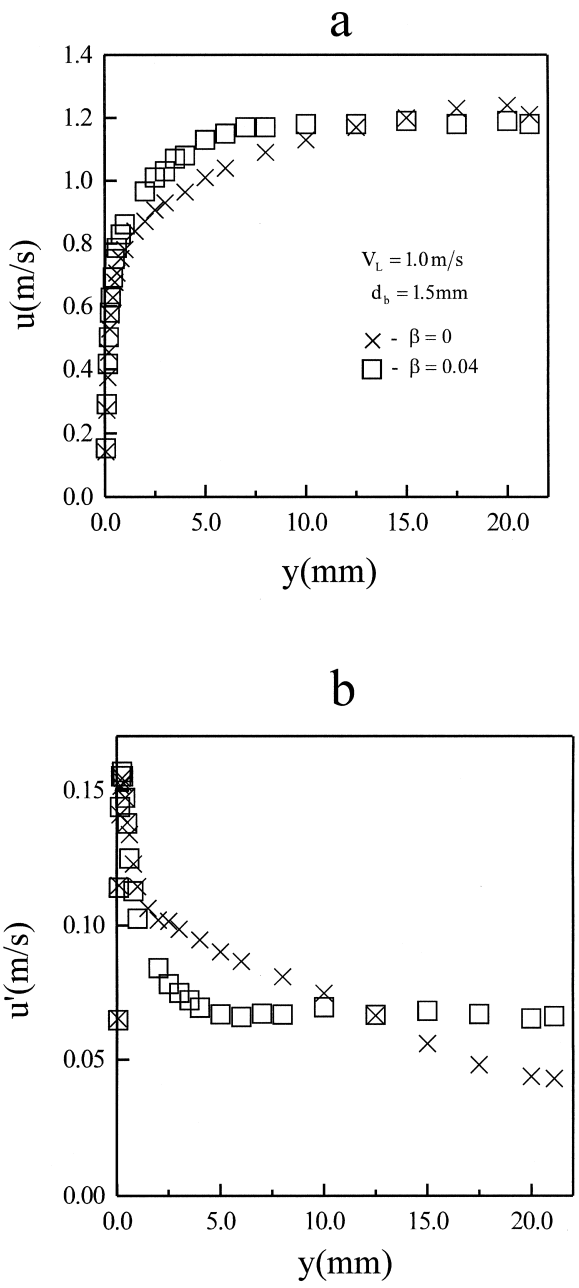

Fig. 32. Mean and fluctuating liquid velocities, $V_L = 1.0$ m/s.

corresponds to the region of velocity fluctuation damping compared to a single-phase flow. Similar behavior can be observed in Fig. 33 for a profile with $V_1 = 0.75$ m/s, $\beta = 0.052$. No single-phase turbulence can be produced in the region with $du/dy = 0$. So all

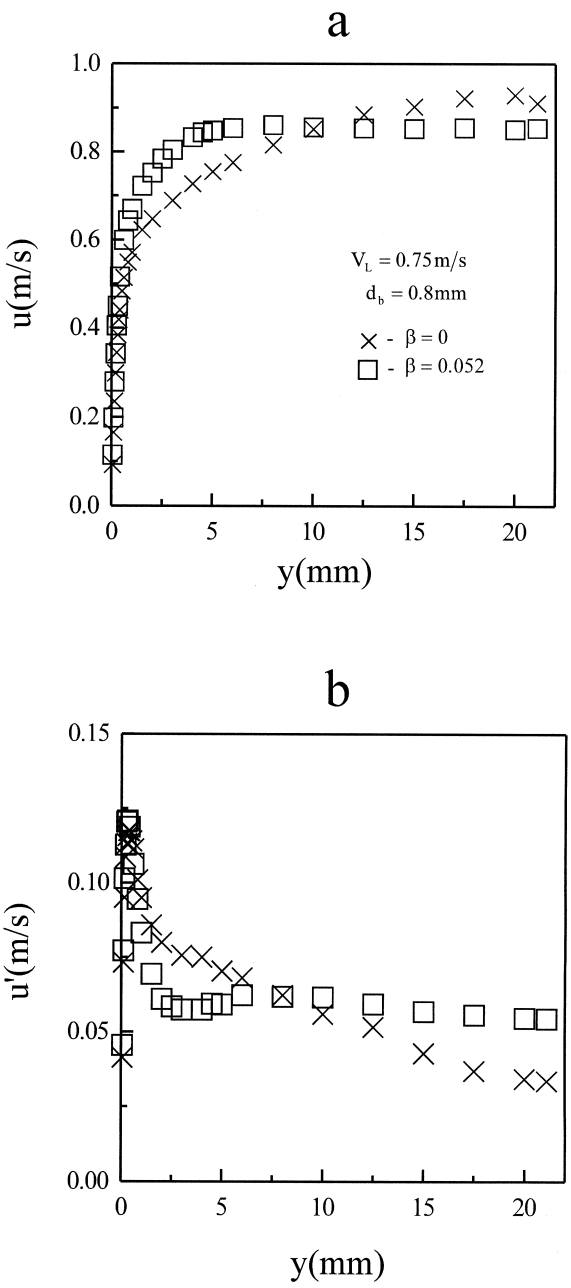

Fig. 33. Mean and fluctuating liquid velocities, V_L = 0.75 m/s.

the turbulence in the central part of the pipe can be attributed to the bubble agitation. The value of u' in the central part of the pipe is constant due to constant local void fraction (Figs. 8–10).

Therefore, the effect of buoyant forces on the flow results in the shear stress decrease compared to single-phase flow, to the velocity profile flattening and to the reduction of liquid velocity fluctuations.

4. Discussion

Comparison of the results obtained on the downward bubbly flow with those reported for upward bubbly flows show that the main difference in the flow structure is the distribution of bubbles over the pipe cross section. Centre-peaked void profiles usually exist in downward flows, the region close to the wall is completely or almost completely free of bubbles. Analysis of the void distributions obtained confirms the suggestion of Zun (1980) that the main reason for the bubble migration in the flow is the lateral force acting on the rising bubble in the flow with the velocity gradient. This force has opposite signs in upflow and downflow due to the different direction of the relative bubble velocity as compared to the liquid velocity. Therefore, centre-peaked profiles were obtained in downflow while in upflow, wall-peaked profiles dominated.

Generally, the bubble size produces effect on the flow parameters. The momentum exchange between liquid and gas depends on bubble diameter and its relative velocity. The relative velocity of bubbles increases with the increase in bubble size. So the momentum exchange increases strongly with the increase of bubble diameter. The effect of bubble size on flow parameters was observed both in upflow and downflow (Gorelik et al., 1987; Valukina et al., 1979).

The mechanism which causes the increase of wall shear stress in downward flow is different from that for upward flow. Nakoryakov et al. (1981) stated that in upward flow, the highest wall shear stress corresponded to the regimes with high bubble concentration near the wall. The bubbles moving close to the wall in the void peak attract the liquid, which results in the increase of near-wall liquid velocity and, hence, the velocity gradient. This mechanism is lacking in downward flow because the bubbles are absent in the wall region. For this reason, the mechanism of wall shear increase in downward flow is different. The reason for this increase is the flattening of the liquid velocity profile in the central part of the pipe. This flattening is much more pronounced in the downward flow compared to the upward one due to higher bubble concentration in the central region. The effect of bubble size on wall shear stress may be attributed to the higher turbulization of the flow by big bubbles for which both the size and the relative velocity are higher.

Non-uniform distribution of void fraction over the pipe section produces the conditions in the flow similar to combined thermal convection. This results in the redistribution of shear stress over the radius and in the flattening of the velocity profile.

There is a well known mecahnism of liquid turbulence suppression which is realized at high liquid velocities (Michiyoshi and Serizawa, 1986; Serizawa and Kataoka, 1990). The limiting case of this mechanism is the deformation of turbulence structure in microbubble-modified turbulent boundary layers. The decrease of velocity and wall shear stress fluctuations observed in downward flow demonstrates the existence of another mechanism of turbulence suppression which is evident at low liquid velocities. It is caused by the mean velocity flattening resulting in

the damping of the turbulent energy production. In this case, the fluctuations decrease at the wall and just close to it. An evident demonstration of this effect was presented by Gorelik et al. (1987) in the experiments on downward bubbly flow in a 15 mm diameter pipe. A strong decrease of wall shear stress and velocity fluctuations was observed for pipes with Reynolds numbers up to 10,000.

5. Conclusions

The following main conclusions can be obtained from the experiments performed: Wall shear stress in downward bubbly flow is higher than in a single-phase flow with the same liquid velocity. The value of the wall shear stress ratio depends strongly on the mean bubble size increasing with larger bubbles. A good correlation with the prediction of Clark and Flemmer (1985a) was observed.

Liquid velocity measurements demonstrated the validity of the single-phase ''law-of-the-wall'' for two-phase velocity profiles. The actual two-phase wall shear stress is an appropriate parameter describing the near-wall velocity distribution.

Turbulence suppression phenomena were observed for downward bubbly flow both for wall shear stress and liquid velocity fluctuations. Reduction of velocity fluctuations compared to the case of single-phase flow was evident when using friction velocity as a scaling parameter.

The aim of further studies is to give some evidence of the physical mechanisms involved in the development of downward flow turbulent structure.

Acknowledgements

The authors express their gratitude to Dr J. L Marie and Prof M. Lance for a fruitful discussion of the results.

This work was partly supported by the International Science Foundation (grant no RBY 300).

References

Antal, S.P., Lahey, R.T., Flaherty, J.E., 1991. Analysis of phase distribution in fully developed laminar bubbly two-phase flow. Int. J. Multiphase Flow 17, 635–652.

Armand, A.A., 1946. Pressure drop in a two-phase flow in horizontal pipes. Izvestia Vsesoyuznogo Teplotekh. Inst. 1, 16–23.

Clark, N.N., Flemmer, R.L.C., 1984. On vertical downward two phase flow. Chem. Engng. Sci. 39, 170–173.

Clark, N.N., Flemmer, R.L.C., 1985a. Two-phase pressure loss in terms of mixing length theory. Ind. Engng. Chem. Fundam. 24, 412–423.

Clark, N.N., Flemmer, R.L.C., 1985b. Predicting the holdup in two-phase bubble upflow and downflow using the Zuber and Findlay drift-flux model. AIChE J. 31, 500–503.

Clark, N.N., Van Egmond, J.W., Nebiolo, E.P., 1990. The drift-flux model applied to bubble columns at low velocity flows. Int. J. Multiphase Flow 16, 261–279.

Drew, D.A., Lahey, R.T., 1982. Phase distribution mechanism in turbulent low-quality two-phase flow in a circular pipe. J. Fluid Mech. 117, 91–106.

Ganchev, B.G., Nizovtzev, V.A., Peresadko, V.G., 1984. Downward bubbly flows at low velocity of phases. Pristenniye Struiniye Potoki. Novosibirsk, Institut Teplofiziki, pp. 85–91.

Ganchev, B.G., Peresadko, V.G., 1985. Hydrodynamic and heat transfer processes in descending bubble flows. J. Engng. Phys. 49, 181–189.

Gorelik, R.S., Kashinsky, O.N., Nakoryakov, V.E., 1987. Study of downward bubbly flow in a vertical pipe. J. Appl. Mech. Techn. Phys. 1, 69–73.

Ibragimov, M.Kh, Bobkov, V.P., Tychinsky, N.A., 1973. Investigation of the behavior of gas phase in a turbulent flow of air-water mixture in channels. Teplofizika Vysokikh Temp. 11, 1051–1061.

Kashinsky, O.N., Gorelik, R.S., Randin, V.V., 1995. Upward bubbly flow in a small-diameter vertical pipe. Russ. J. Engng. Thermophys. 5, 177–193.

Kline, S.J., 1985. The purpose of uncertainty analysis. J. Fluids Engng. 107, 153–160.

Lance, M., Marie, J.L., Bataille, J., 1991. Homogeneous turbulence in bubbly flows. J. Fluids Engng. 113, 295–307.

Liu, T.J., Bankoff, S.G., 1993. Structure of air-water bubbly flow in a vertical pipe. Int. J. Heat Mass Transfer 36, 1049–1060.

Michiyoshi, I., Serizawa, A., 1986. Turbulence in two-phase bubble flow. Nucl. Engng. Design. 95, 253–267.

Marie, J.L., 1987. Modelling of the skin friction and heat transfer in turbulent two-component bubbly flows in pipes. Int. J. Multiphase Flow 13, 309–325.

Marie, J.L., Moursali, E., Tran-Cong, S., 1997. Similarity law and turbulence intensity profiles in a bubbly boundary layer at low void fractions. Int. J. Multiphase Flow 23, 227–247.

Moursali, E., Marie, J.L., Bataille, J., 1995. An upward turbulent bubbly boundary layer along a vertical flat plate. Int. J. Multiphase Flow 21, 107–117.

Nakoryakov, V.E., Kashinsky, O.N., 1995. Gas–liquid bubbly flow in a near-wall region. In: G.P. Celata, R.K. Shah (Ed.). Two-Phase Flow Modelling and Experimentation 1995, 1. Edizioni ETS, Piza, pp. 453–458.

Nakoryakov, V.E., Kashinsky, O.N., Burdukov, A.P., Odnoral, V.P., 1981. Local characteristics of upward gas–liquid flows. Int. J. Multiphase Flow 7, 63–81.

Nakoryakov, V.E., Kashinsky, O.N., Kozmenko, B.K., 1984. Electrochemical method for measuring turbulent characteristics of gas–liquid flows. In: J.M. Delhaye, G. Cognet (Ed.). Measuring Techniques in Gas–liquid Two-Phase Flows. Springer, Berlin, pp. 695–721.

Nakoryakov, V.E., Burdukov, A.P., Kashinsky, O.N., Geshev, P.I., 1986a. Electrodiffusional Method for Studying Local Structure of Turbulent Flows. Institut Teplofiziki, Novosibirsk.

Nakoryakov, V.E., Kashinsky, O.N., Kozmenko, B.K., Gorelik, R.S., 1986b. Study of upward bubbly flow at low liquid velocities. Izvestia SO AN SSSR, Ser. tekh. nauk 3, 15–20.

Oshinovo, T., Charles, M.E., 1974. Vertical two-phase flow. Holdup and pressure drop. Canad. J. Chem. Engng. 52, 438–448.

Sato, Y., Sadatomi, M., Sekoguchi, K., 1981. Momentum and heat transfer in two-phase bubbly flow. Int. J. Multiphase Flow 7, 167–177.

Schlichting, G., 1969. Boundary Layer Theory. McGraw–Hill, New York.

Serizawa, A., Kataoka, I., 1990. Turbulent suppression in bubbly two-phase flow. Nucl. Engng. Design. 122, 1–16.

Serizawa, A., Kataoka, I., Michiyoshi, I., 1975. Turbulent structure of air–water bubbly flows. Int. J. Multiphase Flow 2, 235–246.

Valukina, N.V., Kozmenko, B.K., Kashinsky, O.N., 1979. Characteristics of a flow of monodisperse gas–liquid mixture in a vertical pipe. J. Engng. Phys. 36, 695–699.

Wallis, G.B., 1974. The terminal speed of drops and bubbles in an infinite medium. Int. J. Multiphase Flow 1, 491–511.

Wang, S.K., Lee, S.J., Jones, O.C., Lahey, R.T., 1987. 3-D turbulence structure and phase distribution mechanism in bubbly two-phase flows. Int. J. Multiphase Flow 13, 327–343.

Zun, I., 1980. The transverse migration of bubbles influenced by walls in vertical bubbly flow. Int. J. Multiphase Flow 6, 583–588.